Inorganic Chemistry

ARTICLE

pubs.acs.org/IC

Experimental Study of Decomposition of Aqueous Nitrosyl Thiocyanate

Mark S. Rayson, John C. Mackie, Eric M. Kennedy, and Bogdan Z. Dlugogorski*

Process Safety and Environment Protection Research Group, School of Engineering, The University of Newcastle, Callaghan, NSW 2308, Australia

Supporting Information

ABSTRACT: This study has examined the kinetics of the decomposition of nitrosyl thiocyanate (ONSCN) by stopped flow UV−vis spectrophotometry, with the reaction products identified and quantified by infrared spectroscopy, membrane inlet mass spectrometry, ion chromatography, and CN^- ion selective electrode. The reaction results in the formation of nitric oxide and thiocyanogen, the latter decomposing to sulfate and hydrogen cyanide in aqueous solution. The rate of consumption of ONSCN depends strongly on the concentration of SCN^- ions and is inhibited by nitric oxide. We have developed a reaction mechanism that comprises three parallel pathways for the decomposition of ONSCN. At high thiocyanate concentrations, two reaction pathways operate including a second order reaction to generate NO and $(SCN)_2$ and a reversible reaction between ONSCN and SCN^- producing NO and $(SCN)_2^-$, with the rate limiting step corresponding to the consumption of $(SCN)_2^-$ by reaction with ONSCN. The third reaction pathway, which becomes significant at low thiocyanate concentrations, involves formation of a previously unreported species, ONOSCN, via a reaction between ONSCN and HOSCN, the latter constituting an intermediate in the hydrolysis of $(SCN)_2$. ONOSCN contributes to the formation of NO via homolysis of the O−NO bond and subsequent dimerization and hydrolysis of OSCN. Fitting the chemical reactions of the model to the experimental measurements, which covered a wide range of reactant concentrations, afforded estimation of all relevant kinetic parameters and provided an excellent match. The reaction mechanism developed in this contribution may be applied to predict the rates of NO formation from ONSCN during the synthesis of azo dyes, the gassing of explosive emulsions, or nitrosation reactions occurring in the human body.

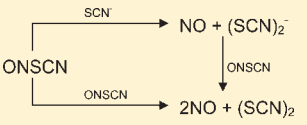

INTRODUCTION

Nitrosation reactions, in which the nitroso (NO^+) group transfers from a reactant to a substrate, are important in a diverse range of industrial, environmental, and biological applications. Industrially, nitrosation reactions play important roles in the synthesis of azo dyes,[1] the production of hydroxylamine,[2] the sensitization of emulsion explosives,[3] and have potential to assist in removal of wax deposits in oil pipelines.[4] In biology, nitrosation reactions have received great attention owing to the importance of S-nitrosothiols as a source of nitric oxide in the human body,[5,6] and the formation of carcinogenic N-nitrosamines, which can occur under acidic conditions in the human body or in the environment.[7−9] Under acidic conditions, nitrosation reactions proceed via the nitrosating agents N_2O_3 and $H_2NO_2^+$, derived from nitrous acid.[10] N_2O_3 serves as the primary nitrosating agent under mildly acidic conditions (pH > 1), while $H_2NO_2^+$ dominates under highly acidic conditions.

$$HNO_2 + NO_2^- + H^+ \rightleftharpoons N_2O_3 + H_2O \quad (1)$$

$$HNO_2 + H^+ \rightleftharpoons H_2NO_2^+ \quad (2)$$

In the presence of added nucleophiles, such as Cl^-, Br^-, I^-, and SCN^-, a new nitrosation pathway operates as a consequence of the formation of nitrosyl halides, denoted ONX (where X = Cl, Br^-, I^-, or SCN^-). The formation of nitrosyl halides catalyzes a wide range of nitrosation reactions, with elevated reaction rates induced by an increase in the concentration of nitrosating agents in the system. Thiocyanate ions, in particular, represent powerful catalysts owing to the large equilibrium constant for the formation of nitrosyl thiocyanate, ONSCN, and in many cases the catalyzed rate of nitrosation can be many orders of magnitude faster than the uncatalyzed rate.[11−15] For a wide variety of substrates, the formation of ONSCN is sufficiently fast for this species to reach its equilibrium concentration as shown below:[16]

$$H^+ + HNO_2 + SCN^- \rightleftharpoons ONSCN + H_2O \quad (3)$$

$$K_{ONSCN} = \frac{[ONSCN]}{[H^+][HNO_2][SCN^-]} \quad (4)$$

The evidence for the existence of ONSCN comes from spectroscopic and kinetic studies, which both indicate the presence of a species formed according to eq 3. Acidic solutions of nitrous acid containing thiocyanate ions display a characteristic red color, the intensity of which depends on the concentrations of H^+, SCN^-, and HNO_2. The red colored species exhibits a broad absorption band with a maximum at 460 nm (ε_{460} = 100 M^{-1} cm^{-1}), and an equilibrium constant of 32 M^{-1} at 25 °C.[17] First-order dependencies of H^+, SCN^-, and HNO_2 concentrations on the rate of catalytic reaction demonstrate that the

Received: December 7, 2010
Published: July 20, 2011

abundance of ONSCN accounts for both the visible absorption and the catalysis of nitrosation reactions by thiocyanate ions.[16]

Our interest in nitrosyl thiocyanate stems from the potential for this species to produce nitric oxide as a side product during thiocyanate-catalyzed nitrosation reactions, in particular, the sensitization of emulsion explosives, wherein thiocyanate ions catalyze the nitrosation of ammonia (from ammonium nitrate) forming small bubbles of nitrogen gas within the explosive. These bubbles undergo adiabatic compression during explosive detonation, acting as hot spots to propagate the explosion front through the bulk explosive.[18] Whereas the sensitization reaction produces primarily N_2, a fraction of the gas generated consists of NO and NO_2, which can pose a safety hazard to miners prior to explosive detonation, particularly when used in confined underground mines.

ONSCN, known to be unstable in pure form, decomposes readily even at temperatures approaching −60 °C to form nitric oxide and thiocyanogen.[19]

$$2\mathrm{ONSCN} \rightarrow 2\mathrm{NO} + (\mathrm{SCN})_2 \qquad (5)$$

Dilute aqueous solutions of ONSCN are relatively stable, however, the red color of the solutions fades over time with evolution of nitric oxide.[20] Despite its widespread applications as a catalyst for nitrosation reactions, to our knowledge, the kinetics and mechanism of ONSCN decomposition have not been studied in detail. Thus, we are interested to determine the kinetics and mechanism of ONSCN decomposition, allowing us to assess the contribution of ONSCN to the formation of NO_x during explosive sensitization. In addition to its industrial applicability, ONSCN has the potential to be a source of nitric oxide in living systems. Knowledge of the mechanism and rate of ONSCN decomposition will enable an assessment of its contribution to NO formation in biological systems. Further to its role as a catalyst for nitrosation reactions, ONSCN has been detected during the oxidation of thiocyanate ions by nitric acid,[21,22] however, the role of ONSCN in the reaction mechanism is unclear. Knowledge of the rate and mechanism of ONSCN decomposition will also assist in elucidating this reaction pathway.

EXPERIMENTAL SECTION

Reagents and Solutions. Sodium nitrite (>99.5%), sodium thiocyanate (>98%), and sodium perchlorate (ACS reagent, 98%) were obtained from Sigma Aldrich, whereas perchloric acid (analytical reagent grade) was purchased from Ajax. Reactant solutions were prepared by dissolving a known mass of solid in distilled deionized water. In the case of NaSCN, the solid was dried in an oven at 150 °C to constant weight before use.[23] Sodium perchlorate was stored in a desiccator to prevent moisture absorption. Solutions of perchloric acid of the desired concentration were produced by diluting 70% $HClO_4$ in distilled deionized water and were standardized by titrating against Na_2CO_3. The ionic strength of all reactant solutions was adjusted to 1 M using $NaClO_4$, except for the initial rates study in which the ionic strength was 2 M.

Nitric oxide (NO) solutions were prepared by first degassing the target solution with N_2 to remove oxygen, prior to bubbling with NO generated via the reduction of nitrous acid by ascorbate.[24] Dissolved NO concentrations were determined by UV absorbance (as nitrite) subsequent to reaction of a small aliquot of NO solution with water containing dissolved oxygen. Results coincided with literature values[25] for NO saturation in water (1.9×10^{-3} M atm^{-1}), and in 1 M $NaClO_4$ (1.2×10^{-3} M atm^{-1}). Further details of this procedure are contained in the Supporting Information.

Instrumental Methods and Procedures. *Kinetics: Stopped Flow UV−vis.* An RX-2000 rapid mixing accessory from Applied Photophysics was coupled to a Varian Cary50 UV−visible spectrometer to study the decomposition kinetics of ONSCN. A constant-temperature circulating bath supplied the water to surround the drive syringes of the RX-2000 and maintain them at a preset temperature. A thermostatted cell holder, regulated by a Varian Cary single-cell Peltier temperature controller, housed the observation cell. All experiments were performed at 298 K. Deoxygenation of reactant solutions was achieved by bubbling with nitrogen gas for at least 15 min, with longer degassing times yielding identical results. Prior to each experiment, we flushed the stopped flow apparatus with deoxygenated water and acquired a baseline absorbance reading, storing it in the Varian software to be automatically subtracted from subsequent measurements. ONSCN was produced in situ, by reacting a dissolved $NaNO_2$ and NaSCN solution with a solution of perchloric acid. The absorbance at 460 nm (ε_{460} = 100 M^{-1} cm^{-1}) served to determine the concentration of ONSCN.

Analysis of Gaseous Products: FTIR and MIMS. Fourier transform infrared spectroscopy (FTIR) of product gases was performed on a Varian IR-600 with 0.5 cm^{-1} resolution and 10 m path length cell (Infrared Analysis Inc.). We generated gas samples in a sealed 50-mL glass reactor initially containing a deoxygenated solution of SCN^- and NO_2^- at pH > 7. Reaction was initiated by addition of a small volume of 2 M $HClO_4$ through a septum side port in the reactor, forming ONSCN in situ. The product gases were purged from the reactor with high-purity nitrogen gas, dried by passage over a column of silica gel and collected in a 3-L gas transfer bag for analysis. Separate experiments established that silica gel did not adsorb NO. Prior to recording a background spectrum, the gas cell was subjected to three cycles of evacuation and filling with high-purity nitrogen. The cell was then loaded with the sample for scanning, with the background automatically subtracted from the sample spectrum by the Varian software. Gases were quantified using the QASoft program (Infrared Analysis Inc.) which applies a region integration and subtraction (RIAS) method to determine the concentrations based on standard spectra from the QASoft database.

The membrane inlet mass spectroscopy (MIMS)[26] experiments employed a Pfeifer Thermostar quadrupole mass spectrometer to detect the gases diffusing from the aqueous solution. A 1-cm length of semipermeable silastic tubing housed the end of the MS capillary, allowing direct measurement of dissolved gases. In these experiments, the solution was degassed with high purity argon to remove oxygen and nitrogen present from air. The purge gas was turned off at the start of the experiment.

Analysis of Aqueous Products: Ion Chromatography and Ion Selective Electrode. Analysis of ionic products was performed on a Dionex DX-100 ion chromatograph with an eluent containing 8 mM Na_2CO_3 and 1 mM $NaHCO_3$, an Ionpac AS14A analytical column and AG14A guard column, with suppressed conductivity detection. We employed the same reactor setup for these experiments as was used for generating gases for the FTIR analysis. In these experiments, HCl functioned to acidify the solution rather than $HClO_4$ due to the incompatibility of ClO_4^- with the IC column. Samples were drawn from the reactor using a gastight syringe via a septum side port and quenched with 0.1 M NaOH to cease the reaction, before being diluted between 20 and 50 times for analysis. Concentrations of NO_2^-, NO_3^-, and SO_4^{2-} were determined by comparing the peak area and retention time of the sample solution to a calibration plot generated using known standards. A Nico2000 cyanide ion selective electrode and double junction reference electrode, connected to a Hanna 213 pH/mV meter via a Nico2000 dual electrode head, determined the cyanide ion concentration after the sample was diluted in 0.1 M NaOH. The electrode

dx.doi.org/10.1021/ic102445d |*Inorg. Chem.* 2011, 50, 7440–7452

system was calibrated with cyanide solutions prepared by dissolving solid NaCN in 0.1 M NaOH and diluting to the appropriate concentration.

Data Analysis. We fitted the measurements for the first 5 min of experiments to potential reaction mechanisms using the DynaFit program.[27] The mechanism was written into a Dynafit script file, and rate constants were included for all known reactions. In the case of protonation equilibria, we followed the same approach as da Silva et al.[28] whereby the association reaction between the hydrogen ion and a negatively charged base (i.e., reaction between NO_2^- and H^+) was assumed to occur with a rate of 10^{10} M^{-1} s^{-1}, with the dissociation reaction rate constant determined from the equilibrium constant. The DynaFit program automatically generates a system of first-order ordinary differential equations describing the reaction mechanism, and fits the rate constants in these equations to minimize the error between the model and the experimental data using a Levenberg−Marquardt algorithm. For each potential mechanism, several initial guesses were trialed to ensure the convergence of the program to a global minimum.

Under the experimental conditions of this study, conversion of HNO_2 to ONSCN is incomplete, and absorbance readings must be corrected for this when determining the overall rate of nitrous acid consumption (or NO generation). Equation 6 relates the concentration of ONSCN to the total nitrous acid concentration:

$$[ONSCN] = \frac{K_{ONSCN}[SCN^-][H^+]}{1 + K_{ONSCN}[SCN^-][H^+]}[HNO_2]_{Total} \quad (6)$$

Under the conditions of the present study, with high H^+ and relatively low nitrous acid concentrations, the concentrations of nitrite ion and dinitrogen trioxide are negligible, and the total nitrous acid concentration is defined according to eq 7.

$$[HNO_2]_{Total} = [HNO_2] + [ONSCN] \quad (7)$$

RESULTS

1. Equilibrium Constant for the Formation of ONSCN. Applying the molar absorptivity of 100 M^{-1} for ONSCN reported by Stedman and Whincup,[17] we determined the equilibrium constant for the formation of nitrosyl thiocyanate at an ionic strength of 1 M as 22.1 ± 0.7 M^{-2}. This value agrees with those of Jones et al.[21] (K_{ONSCN} = 22 M^{-2}) and Bazsa and Epstein[22] (K_{ONSCN} = 20.4 M^{-2}), measured in 1 M perchloric and nitric acids, respectively. Note that K_{ONSCN} constitutes an apparent equilibrium constant as it involves no correction for the effect of nonunity activity coefficients. The apparent molar absorptivity of nitrosyl thiocyanate increases at high thiocyanate ion concentrations. Doherty et al. investigated this increase in absorbance and found it to be consistent with formation of an adduct between SCN^- and ONSCN.

$$ONSCN + SCN^- \rightleftarrows ON(SCN)_2^- \quad (8)$$

The absorbance of $ON(SCN)_2^-$ must be taken into account when determining the concentration of ONSCN, especially at higher SCN^- concentrations where reliance on the 100 M^{-1} cm^{-1} extinction coefficient would result in considerable error. Supporting Information provides further details of these experiments.

2. Reaction Products. The decomposition of pure nitrosyl thiocyanate produces NO and $(SCN)_2$.[19] Aqueous solutions of $(SCN)_2$ are unstable,[29] decaying to form SCN^-, SO_4^{2-}, and HCN (reaction 9). Therefore, if ONSCN decomposition in aqueous solution proceeds with the stoichiometry of reaction 5, the overall stoichiometry of ONSCN disappearance corresponds to that of reaction 10. We therefore attempted to analyze both the aqueous and gaseous reaction products to determine if this is indeed the correct stoichiometry.

$$3(SCN)_2 + 4H_2O \rightarrow 5SCN^- + SO_4^{2-} + HCN + 7H^+ \quad (9)$$

$$6ONSCN + 4H_2O \rightarrow 6NO + 5SCN^- + SO_4^{2-} + HCN + 7H^+ \quad (10)$$

Analysis of Gaseous Reaction Products Using FTIR and MIMS. As quantified by FTIR, nitric oxide accounted for 87% (245 ppm) of the detected gases. A considerable amount of NO_2 also formed, corresponding to 10% (27 ppm) of the products as a result of NO oxidation by a small volume of air contaminating the sample bag. Thus, in complete absence of oxygen, NO would constitute 97% of the gaseous reaction products.

Unexpectedly, we observed a small amount of N_2O, corresponding to 2.5% (7 ppm) of the gaseous products. This result indicates a side reaction leading to N_2O rather than NO, as outlined in the Discussion. A small amount of CO_2 also appeared in the analyzed mixture, corresponding to less than 1% (1.5 ppm) of the gases detected. The very low concentration of CO_2 made it impossible to determine whether CO_2 arises in a side reaction, or whether it results from the liberation of dissolved CO_2/HCO_3^- upon acidification of the reactant solution. The yields of CO_2 and N_2O are sufficiently small that the reactions generating these species have a negligible impact on the overall kinetics of ONSCN decomposition.

The gases were also analyzed by MIMS to determine if any N_2 formed as a product of ONSCN decomposition. The reaction solution was degassed with argon prior to generation of ONSCN via the addition of a small volume of $HClO_4$ to a sealed reactor housing the MIMS probe. The results showed a rapid increase in the ion current at m/z = 30 corresponding to the production of NO. The signal at m/z = 28 remained constant throughout the experiment, indicating that no N_2 formed as a result of ONSCN decomposition.

Analysis of Aqueous Products. Ion chromatography afforded the analysis of the ionic products, with the exception of CN^-, as quantified with an ion selective electrode. The nitrite concentration decreased with increasing decomposition time, owing to the decomposition of ONSCN. Nitrate was detected at concentrations corresponding to less than 1% of the initial nitrite added, with the nitrate concentration initially increasing with time before decreasing slowly. This small amount of nitrate formed from the decomposition of nitrous acid. This process is reversible under the experimental conditions and explains why the concentration of nitrate displays nonmonotonic concentration during experiments.[30]

The concentration of sulfate increased with time, with the final yield enclosed between 75 and 90% of the stoichiometric conversion according to reaction 10, for acid concentrations ranging from 0.18 to 0.33 M. Under the same conditions, the final concentration of cyanide varied from 35 to 50% of that expected for complete conversion according to reaction 10. The results appear very similar to those of a prior study on the oxidation of SCN^- by HNO_3, which also proceeds via an $(SCN)_2$ intermediate.[31] In that study, Stedman and Wincup reported lower than expected yields of sulfate and HCN, findings consistent with a competing reaction between $(SCN)_2$

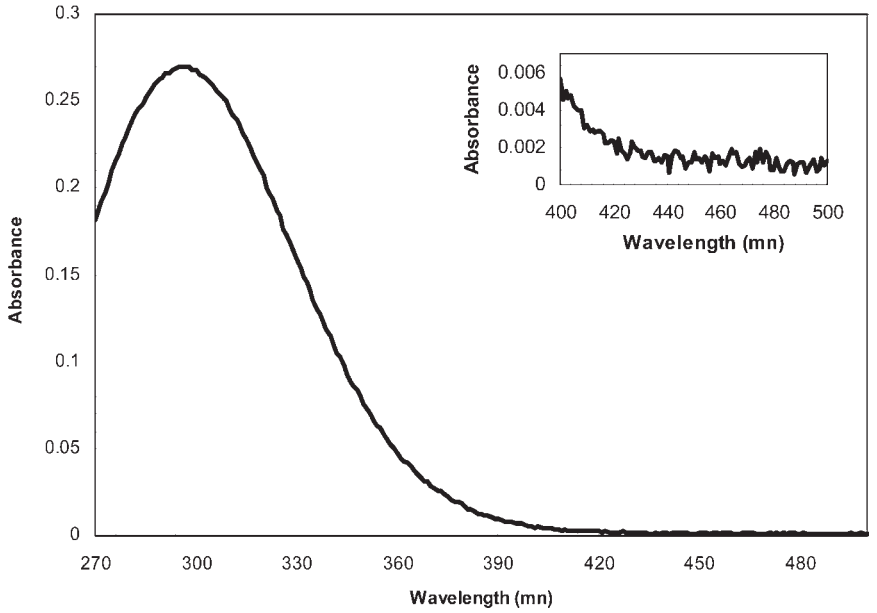

Figure 1. Spectrum of $(SCN)_2$ generated from 0.1 M SCN^-, 1 M $HClO_4$, and 0.9 mM NaClO. The spectrum shown was calculated by subtracting the spectrum after 1 h (at which time $(SCN)_2$ had been almost completely hydrolyzed) from the initial spectrum.

and CN^- forming sulfur dicyanide, $S(CN)_2$.

$$(SCN)_2 + CN^- \rightarrow S(CN)_2 + SCN^- \qquad (11)$$

During the initial stages of reaction, when the concentration of HCN is low, the formation of HCN and sulfate advances in accordance with reactions 9 and 10, which strongly suggests the intermediacy of $(SCN)_2$.

3. Spectrum of Intermediate Species. The formation of sulfate and cyanide ions suggests that ONSCN decomposition proceeds through an $(SCN)_2$ intermediate. $(SCN)_2$ has been identified as a product of the oxidation of SCN^- by a variety of oxidizing species, including H_2O_2,[32] HNO_3,[31] ClO_2,[33] and HOCl,[34] and has a UV spectrum with an absorption maximum near 290 nm. By following the procedure outlined by Barnett et al.,[29] we recorded the spectrum of $(SCN)_2$ to confirm that it did not extend into the visible region where it might interfere with the absorbance of ONSCN, and to aid in identifying $(SCN)_2$ as a reaction intermediate. This involved the oxidation of a NaSCN solution by acidified NaOCl to generate $(SCN)_2$ as shown below:

$$HOCl + 2SCN^- + H^+ \rightarrow (SCN)_2 + Cl^- + H_2O$$
$$(\text{or equivalently } Cl_2 + 2SCN^- \rightarrow (SCN)_2 + 2Cl^-) \qquad (12)$$

The reaction was performed with 1 M $HClO_4$, 0.9 mM NaOCl, and SCN^- concentrations of 0.1 and 0.2 M, conditions leading to reasonably stable solutions of $(SCN)_2$ and reliable measurements of its spectrum. Figure 1 confirms a negligible absorbance of $(SCN)_2$ above 420 nm that does not interfere with the measurements acquired at 460 nm, the absorbance maximum of ONSCN.

Nonuniform changes to the spectra of decomposing ONSCN solutions indicated the formation of a UV absorbing species not present at the start of the experiments. To isolate the spectrum of the intermediate, we subtracted the spectrum of SCN^- and assumed that species in equilibrium with nitrous acid (e.g., HNO_2, ONSCN, and $ON(SCN)_2^-$) accounted exclusively for the initial absorbance. In the absence of additional absorbing species, the decomposition of ONSCN should therefore result in a consistent decrease in absorbance across all wavelengths. This was the case only for wavelengths above 400 nm, with absorbance at lower wavelengths decreasing at a slower rate. Assuming that ONSCN was solely responsible for the absorption at 460 nm, the additional absorbance caused by the reaction intermediate at other wavelengths was calculated and compared to that of $(SCN)_2$ in Figure 2, after scaling the spectrum to a common absorbance. The spectrum of the intermediate concurs with the spectrum of $(SCN)_2$ generated in the independent experiment, indicating that $(SCN)_2$ indeed represents the observed intermediate. The absorbance of the intermediate below 310 nm exceeds that of $(SCN)_2$, suggesting the presence of an additional species absorbing in this region. However, the data at these wavelengths display considerable scatter, induced by high absorbance of ONSCN, which confined the measurements to wavelengths longer than 300 nm.

4. Effect of Initial Dissolved Oxygen on Reaction Kinetics. Initial kinetic experiments with solutions that had not been degassed exhibited an induction period of slow decomposition during the early stages. Bubbling nitrogen gas through the reactant solutions for 15 min prior to starting the reaction removed the induction period, as demonstrated in Figure 3. The induction period arises as a consequence of dissolved oxygen, initially present in the solutions from the atmosphere, reacting with nitric oxide to form NO_2. NO_2 combines with NO and water to regenerate nitrous acid, and as nitrous acid exists in equilibrium with ONSCN, the concentration of ONSCN remains unchanged, as illustrated in Scheme 1.

Therefore, to avoid complications owing to dissolved oxygen, we degassed all reactant solutions by bubbling high-purity nitrogen for at least 15 min. This was sufficient to remove the induction period, however, some experiments showed a miniscule but noticeable rise in the curve suggesting a residual contamination of the solutions by a minute amount of oxygen. This rise, which

dx.doi.org/10.1021/ic102445d |*Inorg. Chem.* 2011, 50, 7440–7452

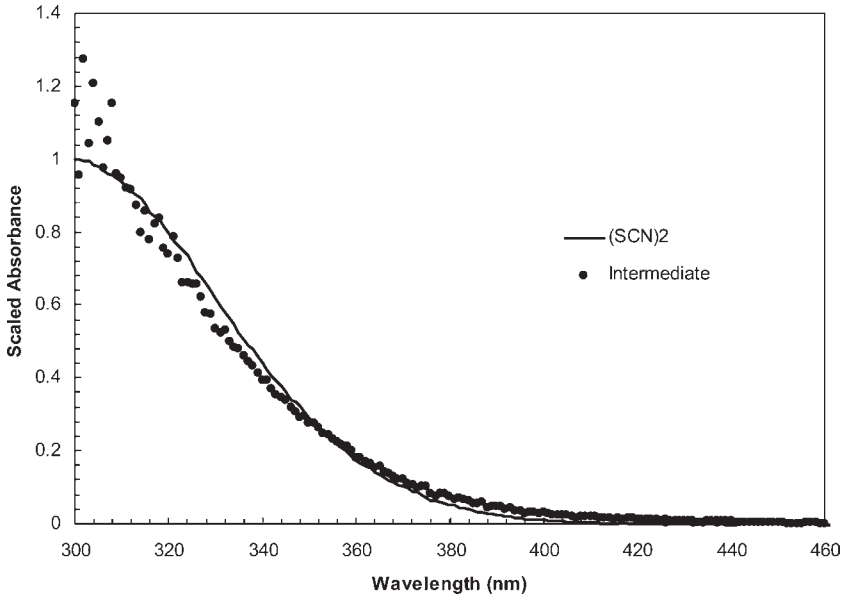

Figure 2. Comparison of spectrum of intermediate species and $(SCN)_2$; intermediate spectrum from experiment with 3 mM $NaNO_2$, 0.2 M $HClO_4$, and 0.2 M NaSCN.

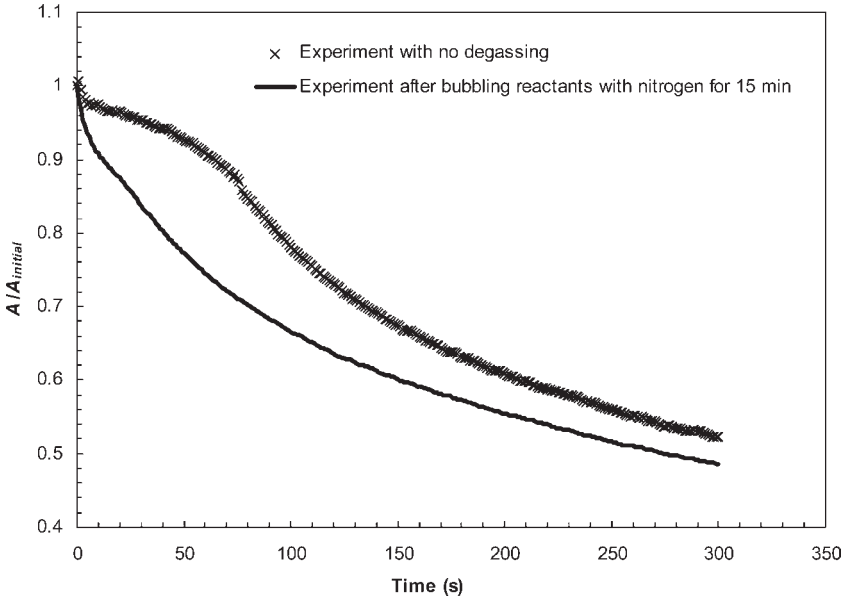

Figure 3. Effect of oxygen on ONSCN decomposition, λ = 460 nm. Both experiments started with 1 mM $NaNO_2$, 1 M $HClO_4$, and 0.1 M NaSCN.

Scheme 1. Regeneration of ONSCN via Oxidation of NO by O_2

$$2ONSCN \rightarrow 2NO + (SCN)_2 \quad (1.1)$$

$$2NO + O_2 \rightarrow 2NO_2 \quad (1.2)$$

$$NO + NO_2 + H_2O \rightarrow 2HNO_2 \quad (1.3)$$

$$HNO_2 + SCN^- + H^+ \leftrightarrows ONSCN + H_2O \quad (1.4)$$

was not reproducible and was not removed by degassing for longer time periods, arises because of diffusion of a small amount of O_2 through the fluorinated ethylene propylene (FEP) tubing in the stopped flow device. This phenomenon appears to have no effect on the overall kinetics and was neglected in the kinetic analysis.

5. Kinetics: Initial Rates and Effect of Thiocyanate Ion Concentration. ONSCN was generated in situ via the reaction of $HClO_4$, SCN^-, and NO_2^- ions. To assist in the development of the mechanism, we studied the initial rates of ONSCN decomposition as a function of the concentrations of nitrous acid and thiocyanate ions. A number of issues complicated this part of our investigation, limiting the quality and usefulness of the initial rates measurements to identifying the early decomposition mechanism and the inhibitory effect of NO on the reaction (described in Section 6). For this reason, the measurements of initial rates did not serve to fit the kinetic

dx.doi.org/10.1021/ic102445d |*Inorg. Chem.* 2011, 50, 7440–7452

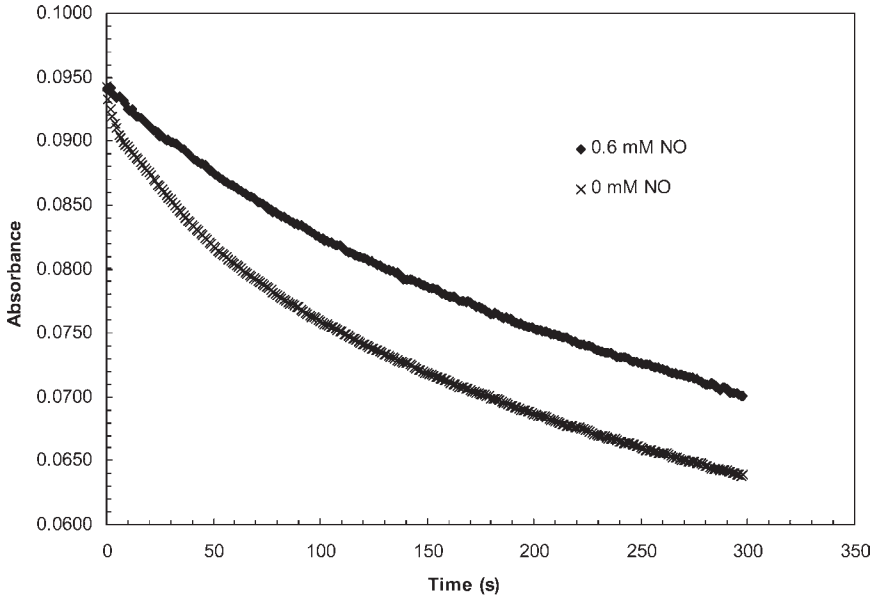

Figure 4. Effect of nitric oxide on ONSCN decomposition, λ = 460 nm. Both experiments contain 3 mM $NaNO_2$, 0.2 M $HClO_4$, and 0.1 M NaSCN.

parameters of the model. The first problem involved the absorbance increasing slightly over the first 200 ms of reaction, as opposed to an expected decrease. This increase was not reproducible, suggesting inefficient mixing in the hand-driven stopped flow device. The second problem comprised the rate remaining constant only for a very short period of time (<1 s) before commencing to decrease rapidly, leading to a small change in absorbance. The resulting initial rate measurements displayed a significant uncertainty, owing to the large noise in the measurements relative to the change in absorbance, and to the irreproducible nature of the early increase in absorbance.

In the first set of experiments (see Supporting Information), the nitrous acid concentration was varied from 1 to 4 mM in increments of 1 mM, with concentrations of 1 and 0.1 M $HClO_4$ and NaSCN, respectively. Under these conditions, with a large excess of SCN^- and H^+, the concentration of ONSCN becomes directly proportional to the concentration of nitrous acid. Using higher concentrations of nitrous acid engendered interference from the decomposition of nitrous acid, which is initially very rapid. Plotting the log of the initial rate versus the log of the HNO_2 concentration indicated a reaction order with respect to nitrous acid of 1.07 ± 0.09. In the second series of experiments, the concentration of SCN^- was varied from 0.1 to 0.25 M in increments of 0.05 M, with constant concentrations of HNO_2 and $HClO_4$ of 2 mM and 1 M, respectively. Under these conditions, the fraction of initial nitrous acid converted into ONSCN ranges from 0.77 to 0.9. The order with respect to SCN^- amounted to 1.2, however, the slight elevation in ONSCN concentration induced a portion of the rate increase. The initial rate was corrected for the effect of the increased ONSCN concentration, assuming that the initial rate was first-order in ONSCN, resulting in an order in SCN^- of 1.06 ± 0.16. Thus, a process first-order in nitrous acid and first-order in SCN^- dominates the initial rate of decomposition of ONSCN, as described by eq 13, assuming that ONSCN accounts for the term first-order in nitrous acid, where k = 0.28 M^{-1} s^{-1} gives the best fit to the measurements.

$$-\frac{d[HNO_2]_{Total}}{dt} = k[ONSCN][SCN^-] \quad (13)$$

6. Kinetics: Effect of Nitric Oxide. The rate of ONSCN decomposition decreases rapidly with time, despite only relatively small changes in ONSCN concentration. This decrease resulted from the inhibition of the reaction by one of the reaction products, either $(SCN)_2$ or NO. It was impossible to test directly for inhibition of ONSCN decomposition by $(SCN)_2$, owing to the instability of $(SCN)_2$ in aqueous solution. However, we readily generated stable NO solutions by passing NO gas through the solution of interest and ensuring that oxygen was strictly excluded during generation and transfer of the solution. Our approach involved examining the effect of NO on the decomposition of ONSCN, by first saturating the reactant solution containing SCN^- and NO_2^- with NO before reacting it with $HClO_4$ in the stopped flow apparatus. Figure 4 illustrates the results of a typical experiment, confirming that the solution initially saturated with NO exhibits significantly slower decomposition of ONSCN. Whereas the solution without NO exhibited a rapid decrease in the rate over time, the solution with NO decomposed at a much steadier and considerably slower rate. This result appears qualitatively very similar to decomposition of nitrosothiourea,[35,36] which is also inhibited by NO.

The fact that NO suppresses the initially rapid decomposition of ONSCN, yet the slope decreases at a steady rate suggests a combination of reversible and irreversible reaction steps in the mechanism. The presence of NO suppresses the reversible step, responsible for the initial rapid decrease in ONSCN concentration, while similar slopes of both curves at 300 s indicate other pathways, or subsequent reaction steps that remain unaffected by NO. Figure 5 illustrates plots of $1/[HNO_2]_{Total}$ versus t, with their linearity after the first 350 s revealing a second-order

dx.doi.org/10.1021/ic102445d |*Inorg. Chem.* 2011, 50, 7440–7452

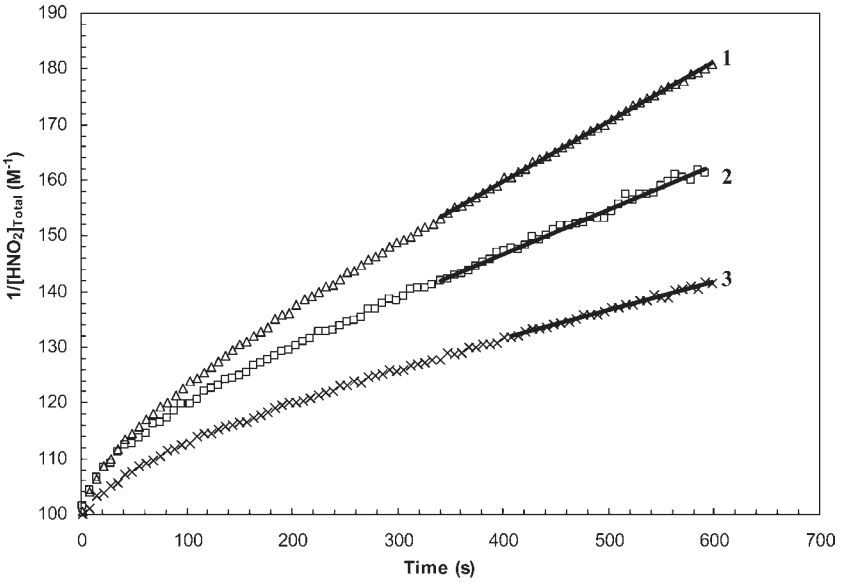

Figure 5. Second-order plots of ONSCN decomposition. All experiments initially contain 0.01 M HNO_2 and 0.05 M NaSCN. $HClO_4$ concentrations are 0.4, 0.3, and 0.2 M for experiments 1, 2, and 3, respectively.

Table 1. Reaction Mechanism for ONSCN Decomposition

reaction	equation number	k_f	k_b	source
$HNO_2 + H^+ + NO_2^- \rightleftarrows N_2O_3 + H_2O$	1	32000 $M^{-2}s^{-1}$	6400 s^{-1}	ref 28
$HNO_2 + H^+ + SCN^- \rightleftarrows ONSCN + H_2O$	3	11900 $M^{-2}s^{-1}$	530 s^{-1}	ref 16
$2ONSCN \rightarrow 2NO + (SCN)_2$	5	**0.57 $M^{-1}s^{-1}$**	**N/A**	**this study**
$SCN^- + ONSCN \rightleftarrows NO + (SCN)_2^-$	14	**2.3 $M^{-1}s^{-1}$**	**4.3×10^9 $M^{-1}s^{-1}$**	**this study, ref** 37
$(SCN)_2^- + ONSCN \rightarrow NO + (SCN)_2 + SCN^-$	15	**1.9×10^7 $M^{-1}s^{-1}$**	**N/A**	**this study, ref** 37
$(SCN)_2^- + HNO_2 + H^+ \rightarrow NO + (SCN)_2 + H_2O$	18	**12000 $M^{-2}s^{-1}$**	**N/A**	**this study**
$(SCN)_2 + H_2O \rightleftarrows HOSCN + SCN^- + H^+$	20	19.8 s^{-1}	5140 $M^{-2}s^{-1}$	ref 23
$ONSCN + HOSCN \rightleftarrows ONOSCN + H^+ + SCN^-$	21	**260 $M^{-1}s^{-1}$**	**980 $M^{-2}s^{-1}$**	**this study**
$ONOSCN \rightleftarrows NO + OSCN$	22	**1.3×10^6 $M^{-1}s^{-1}$**	**4.3×10^9 $M^{-1}s^{-1}$**	**this study**
$2OSCN + H_2O \rightarrow HOSCN + HO_2SCN$	23	**1.7×10^7 $M^{-1}s^{-1}$**	**N/A**	**this study**
$2HOSCN \rightarrow HO_2SCN + SCN^- + H^+$	24	1600 $M^{-1}s^{-1}$	N/A	ref 29[a]
$2HO_2SCN \rightarrow HOSCN + HO_3SCN$	25	2×10^8 $M^{-1}s^{-1}$	N/A	ref 33
$HO_3SCN + H_2O \rightarrow SO_4^{2-} + HCN + 2H^+$	26	5×10^8 $M^{-1}s^{-1}$	N/A	ref 33
$2(SCN)_2^- \rightarrow (SCN)_2 + 2SCN^-$	27	1.3×10^9 $M^{-1}s^{-1}$	N/A	ref 39
$NO_2^- + H^+ \rightleftarrows HNO_2$	28	10^{10} $M^{-1}s^{-1}$	6.76×10^6 s^{-1}	ref 28
$N_2O_3 \rightleftarrows NO + NO_2$	29	3941 s^{-1}	1.0×10^8 $M^{-1}s^{-1}$	refs 40 and 30[b]
$2NO_2 + H_2O \rightarrow HNO_2 + NO_3^- + H^+$	30	8.4×10^7 $M^{-1}s^{-1}$	5×10^{-3} $M^{-2}s^{-1}$	ref 30
$(SCN)_2^- + NO_2^- \rightarrow 2SCN^- + NO_2$	31	2.2×10^6 $M^{-1}s^{-1}$	N/A	ref 41

[a] The value of K_{20} from ref 23 was used in conjunction with the value of $K_{20}{}^2k_{24}$ from ref 29 to determine k_{24}. [b] The value of k_{28} was determined from ref 40 in conjunction with the equilibrium constant for N_2O_3 from ref 28 k_{-28} was taken as the average of values reported in refs 40 and 30.

reaction in total nitrous acid concentration, largely independent of NO concentration.

Reaction Mechanism: Global Kinetic Fit. The initial rates study has identified the early decomposition of ONSCN to be first order in both ONSCN and SCN^- and has demonstrated the reaction to be inhibited by nitric oxide. As the starting rate remained valid only for the first second or so of reaction, we excluded the results of initial rates experiments when deriving the kinetic parameters. Potential models were fitted to a set of 20 experiments simultaneously, each executed for 300 s, with the experiments covering a reasonably wide range of HNO_2, SCN^-, and H^+ concentrations including some with solutions initially saturated with nitric oxide. Thus, $[HNO_2]_{Total}$ ranged from 2 to 10 mM, $[SCN^-]$ from 0.05 to 0.5 M and $[H^+]$ from 0.02 to 0.5 M. This approach allowed the inclusion of the decomposition of HNO_2 in the model, by incorporating appropriate equations and rate constants from the literature (Table 1, reactions 28−30). Table S3 in the Supporting Information provides the initial conditions of each experiment.

dx.doi.org/10.1021/ic102445d |*Inorg. Chem.* 2011, 50, 7440–7452

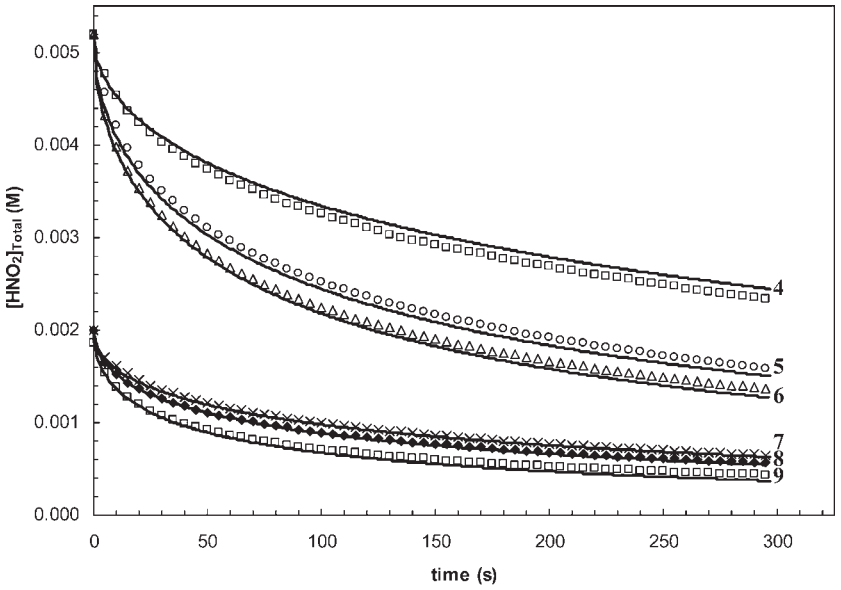

Figure 6. Comparison of experimental data and kinetic model (reactions 14−16) for selected experiments with high thiocyanate ion concentrations. Data points correspond to experimental measurements and solid curves correspond to the best fit of Pathways 1 and 2 to the data set of 10 experiments with $[SCN^-] \geq 0.2$ M. Conditions are 4: $[SCN^-] = 0.3$ M, $[H^+] = 0.1$ M, 5: $[SCN^-] = 0.3$ M, $[H^+] = 0.3$ M, 6: $[SCN^-] = 0.3$ M, $[H^+] = 0.5$ M, 7: $[SCN^-] = 0.3$ M, $[H^+] = 0.3$ M, 8: $[SCN^-] = 0.3$ M, $[H^+] = 0.5$ M, 9: $[SCN^-] = 0.5$ M, $[H^+] = 0.5$ M.

Kinetics at High SCN^- Concentration. At thiocyanate concentrations of 200 mM or higher, the kinetics of ONSCN decomposition comprises two parallel reaction pathways. Pathway 1, denoted as the thiocyanate-dependent pathway, involves reaction between nitrosyl thiocyanate and thiocyanate ions producing nitric oxide and $(SCN)_2^-$ radicals (eq 14), followed by rate-limiting consumption of $(SCN)_2^-$ forming NO and thiocyanogen, $(SCN)_2$ (eq 15). Pathway 2 consists of a second-order reaction in nitrosyl thiocyanate, which produces two molecules of NO and one of thiocyanogen.

Pathway 1.

$$ONSCN + SCN^- \rightleftharpoons (SCN)_2^- + NO \quad (14)$$

$$(SCN)_2^- + ONSCN \rightarrow NO + (SCN)_2^- \quad (15)$$

Pathway 2.

$$2ONSCN \rightarrow 2NO + (SCN)_2 \quad (5)$$

Provided that reaction 14 governs the early rate, this mechanism is consistent with our initial rates study, which highlighted a reaction first order in both ONSCN and SCN^-. Reaction 14 might be expected to be rate limiting initially, when the concentration of NO remains low. Czapski et al.[37] studied the reverse of reaction 14, the reaction between NO and $(SCN)_2^-$, by monitoring the decay of $(SCN)_2^-$ produced via the pulse radiolysis of SCN^- solutions containing NO. They reported k_{-14} as 4.3×10^9 M^{-1} s^{-1}, and we have adopted this value in our simulations. We fitted the kinetic parameters of reactions 5, 14, and 15 to the measurements at high $[SCN^-]$, in conjunction with relevant equations for formation of ONSCN, and for the protonation and decomposition of nitrous acid as outlined in Table 1. For values of $10^5 < k_{15} < 10^8$ M^{-1} s^{-1}, the simulations were insensitive to changes in k_{14} and k_{15} provided that the product $K_{14}k_{15}$ remained constant. A value of $K_{14}k_{15}$ of 1.15×10^{-2} M^{-1} s^{-1} in conjunction with $k_{16} = 0.5$ M^{-1} s^{-1} afforded a good match to the acquired measurements. Figure 6 shows the best fit of reactions 5, 14, and 15 to the results of selected experiments, characterized by initial concentrations of SCN^- in excess of 200 mM. The Supporting Information provides additional graphs for other high $[SCN^-]$ experiments.

Kinetics at Low SCN^- Concentrations. At thiocyanate concentrations below 200 mM, the decomposition of ONSCN displayed faster kinetics than would be expected from Pathways 1 and 2, indicating the presence of an additional reaction pathway operating under these conditions. A variety of different reaction schemes were considered, with three potential mechanisms for ONSCN decomposition found to provide similarly good fits to the data. All three mechanisms contain Pathways 1 and 2 in conjunction with an additional reaction channel. These additional pathways include (i) the homolysis of ONSCN followed by rapid reaction of SCN radicals to form $(SCN)_2^-$, (ii) the nitrosation of $(SCN)_2^-$ by $NO^+/H_2NO_2^+$ forming NO and $(SCN)_2$, or (iii) the nitrosation of HOSCN (formed from $(SCN)_2$ hydrolysis) to produce ONOSCN, and subsequent decomposition of this species. These pathways are outlined below.

Pathway 3(i).

$$ONSCN \rightleftharpoons NO + SCN \quad (16)$$

$$SCN + SCN^- \rightarrow (SCN)_2^- \quad (17)$$

Pathway 3(ii).

$$(SCN)_2^- + HNO_2 + H^+ \rightarrow NO + (SCN)_2 + H_2O \quad (18)$$

Assuming that the rate limiting step in Pathways 3(i) and 3(ii) is the consumption of $(SCN)_2^-$, the following simplified rate law can be derived for ONSCN decomposition, where $k_a = k_{15}k_{16}/k_{-14}$ for pathway 3(i) and $k_{18}K_{14}/K_3$ for pathway 3(ii) (derivation

dx.doi.org/10.1021/ic102445d |*Inorg. Chem.* 2011, 50, 7440–7452

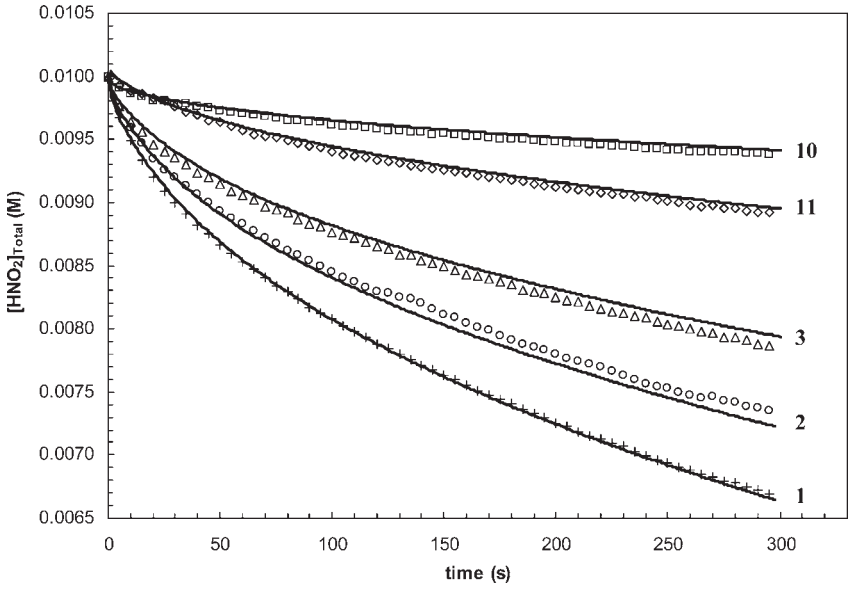

Figure 7. Comparison of experimental and modeled decomposition of ONSCN for 0.05 mM NaSCN, 0.01 M $NaNO_2$ and increasing initial acid concentrations, 0.05, 0.1, 0.2, 0.3, and 0.4 M $HClO_4$ for experiments 10, 11, 3, 2, and 1 respectively. Experiment numbers correspond to those tabulated in the Supporting Information.

provided in the Supporting Information):

$$-\frac{d[HNO_2]_{Total}}{dt} = \frac{k_a[ONSCN]^2}{[NO]} + \frac{k_{15}K_{14}[SCN^-][ONSCN]^2}{[NO]} + k_5[ONSCN]^2 \quad (19)$$

SCN radicals are known to react at or near the diffusion-controlled limit with SCN^- ions forming $(SCN)_2^-$ radicals,[38] with an equilibrium constant of 2×10^5 M^{-1}. Thus, in accordance with Hess' Law, the equilibrium constants for reactions 14 and 16 must satisfy the relationship $K_{14}/K_{16} = K_{17} = 2 \times 10^5$ M^{-1}. The best fit of Pathway 3(i) (occurring in parallel with Pathways 1 and 2) to the data resulted in $K_{14}/K_{16} = 10$, a factor of 10^4 lower than required thermodynamically. Therefore, although this reaction model provides an excellent fit to the data, the required equilibrium parameters are not thermodynamically feasible and alternate mechanisms must be considered. As noted above, Pathway 3(ii) simplifies to the same rate law as Pathway 3(i), with the distinguishing feature of that mechanism being an acid-catalyzed reaction between $(SCN)_2^-$ (generated via reaction 14) and nitrous acid. Such a reaction would likely proceed via a $H_2NO_2^+$ intermediate, making it possible to estimate an upper bound on this rate constant based on the observed rate of other acid-catalyzed nitrosation reactions involving negatively charged substrates. The rate constants of such reactions, including the nitrosation of SCN^- appear to approach a limiting value of 12 000 M^{-2} s^{-1} with increasing substrate reactivity.[16] Hence, the rate of nitrosation of $(SCN)_2^-$ is unlikely to exceed this value. The fact that similar rate constants are observed for a range of reactive substrates suggests that these reactions are encounter controlled, with $H_2NO_2^+$ in equilibrium with HNO_2 and H^+. In contrast, the minimum value of k_{18} required to fit the data for ONSCN decomposition at low SCN^- concentrations is 6.5×10^5 M^{-2} s^{-1}, which is significantly larger than that observed for other substrates. As a result, Pathway 3(ii), although providing a good fit to the data, is unlikely to represent the correct mechanism because the required rate constant for reaction 18 is not feasible.

Pathway 3(iii) involves formation of a previously unreported species, ONOSCN resulting from the nitrosation of HOSCN. HOSCN forms as a result of the hydrolysis of $(SCN)_2$ (reaction 20),[23] produced from Pathways 1−2. HOSCN can then either disproportionate via a second-order reaction which results eventually in sulfate and cyanide (reactions 24−26 in Table 1),[29] or it can react with ONSCN, forming ONOSCN (reaction 21). The decomposition of ONOSCN is proposed to form NO and OSCN radicals via reaction 22. Two OSCN molecules then combine to form a dimer, which hydrolyzes forming HOSCN and HO_2SCN. This reaction scheme, combined with Pathways 1 and 2 operating in parallel, provides an excellent fit to the data over the complete range of reactant concentrations used in this study, as outlined in Figures 7−9. Table 1 summarizes the complete model and associated rate parameters.

Pathway 3-(iii).

$$(SCN)_2 + H_2O \rightleftarrows HOSCN + SCN^- + H^+ \quad (20)$$

$$ONSCN + HOSCN \rightleftarrows ONOSCN + SCN^- + H^+ \quad (21)$$

$$ONOSCN \rightleftarrows NO + OSCN \quad (22)$$

$$2OSCN + H_2O \rightarrow HOSCN + HO_2SCN \quad (23)$$

DISCUSSION

Pathway 1 - Reactions 14 and 15. Pathway 1 involves a reaction between nitrosyl thiocyanate and thiocyanate ions

dx.doi.org/10.1021/ic102445d |*Inorg. Chem.* 2011, 50, 7440–7452

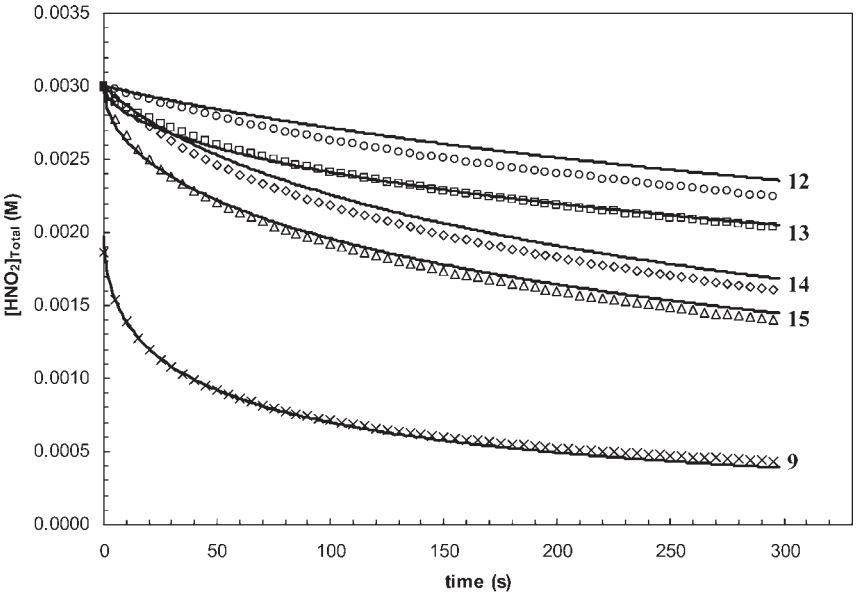

Figure 8. Comparison of experimental and modeled decomposition of ONSCN at low $NaNO_2$ concentrations. Concentrations are 9: $[SCN^-] = 0.5$, $[H^+] = 0.5$, 12: $[SCN^-] = 0.1$ M, $[H^+] = 0.2$, $[NO] = 0.62$ mM, 13: $[SCN^-] = 0.1$ M, $[H^+] = 0.2$, 14: $[SCN^-] = 0.2$ M, $[H^+] = 0.2$, $[NO] = 0.62$ mM, 15: $[SCN^-] = 0.2$ M, $[H^+] = 0.2$ M.

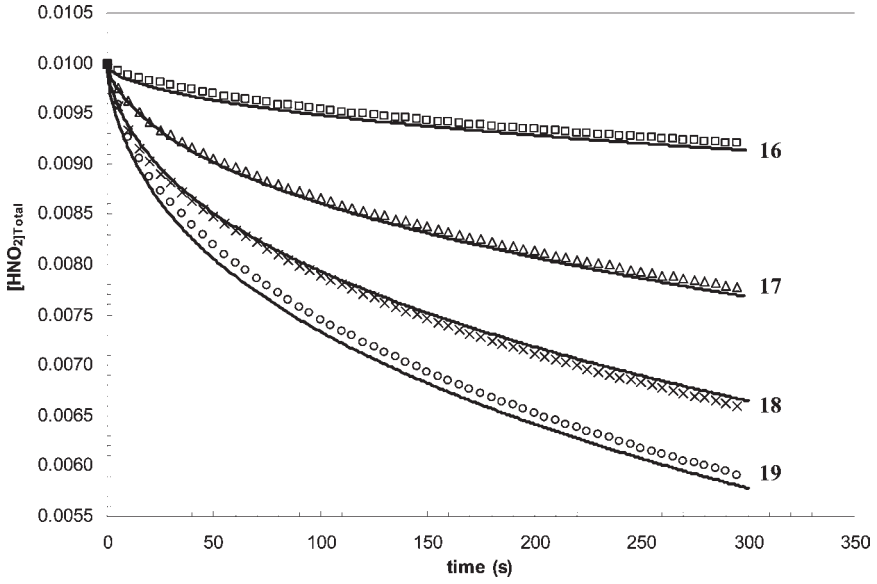

Figure 9. Comparison of experimental and modeled decomposition of ONSCN for experiments 16: $[H^+] = 0.02$ M,$[SCN^-] = 0.2$ M, and 17−19: $[H^+] = 0.1$ M, $[SCN^-] = 0.1$, 0.15, 0.2 M respectively.

generating $(SCN)_2^-$ radicals. This reaction is analogous to those reported for decomposition of other nitroso-species, including nitroso-thioureas[36] and nitrosyl iodide,[42] which feature a reaction between the nitroso compound and the relevant nucleophile. The fact that similar reactions operate for other nitroso species supports the proposed mechanism for ONSCN decomposition, and may indicate a general mechanism applicable for this class of compounds. With regard to the elementary mechanism of this reaction, our measurements and the results of studies published in the literature indicate that the reaction between ONSCN and SCN^- likely proceeds through an $ON(SCN)_2^-$ intermediate. A species of this stoichiometry formed as a result of pulse radiolysis of nitric oxide saturated thiocyanate solutions[37] (i.e., the reverse of reaction 14). Doherty at al. proposed a species of the same stoichiometry, denoted $ON(SCN)_2^-$ to explain the visible spectrum of nitrosyl thiocyanate solutions containing very high thiocyanate ion concentrations.[20] These researchers claimed that this species differs from the species denoted $NO(SCN)_2^-$ observed in pulse radiolysis experiments, and that Czapski et al.[37] had observed a different form of ONSCN. This distinction results from the differences in the UV spectra of ONSCN and NOSCN, and the rapid rate of decay of $NO(SCN)_2^-$, which, according to Doherty et al., would cause the species to "have completely decomposed long before our first measurements,

dx.doi.org/10.1021/ic102445d |*Inorg. Chem.* 2011, 50, 7440–7452

even with stopped flow". The latter point seems somewhat tenuous considering that Doherty et al. measured an equilibrium concentration of $ON(SCN)_2^-$, thus despite having a rapid rate of decay, $ON(SCN)_2^-$ would still be observable provided the rate of its formation exhibited a comparable magnitude to that of its consumption. The small equilibrium constant ($\sim$0.036 M^{-1}) for formation of the $ON(SCN)_2^-$ adduct would mean that under the conditions of Czapski et al.'s experiments with 0.1 M SCN^-, the equilibrium concentration of $ON(SCN)_2^-$ would be very low and its absorbance indistinguishable from ONSCN considering their similar UV spectra. As such, one cannot conclude whether the species observed in these studies are indeed different. Provided that $ON(SCN)_2^-$ exists at equilibrium with ONSCN and SCN^-, the reaction proceeding via $ON(SCN)_2^-$ remains kinetically indistinguishable from that producing NO and $(SCN)_2^-$ from ONSCN and SCN^- in a single step. Doherty et al.[20] showed that $ON(SCN)_2^-$ formation reached equilibrium within the dead time of their stopped flow, thus, we have defined this rate constant in terms of ONSCN and SCN^-.

The simulations were insensitive to changes in k_{14} and k_{15} for $10^5 < k_{15} < 10^8$ $M^{-1}s^{-1}$, provided that the magnitude of $K_{14}k_{15}$ remained constant. The constancy of this quantity can be readily explained by the fact that the rate of reaction 14 is significantly faster than reaction 15. As such, NO and $(SCN)_2^-$ exist in equilibrium with ONSCN and SCN^-, and the rate limiting reaction step is the consumption of $(SCN)_2^-$ via reaction 15. Therefore, under conditions where reaction 14 is at equilibrium, it is not possible to isolate the parameters k_{14} and k_{15}, only $K_{14}k_{15}$ can be determined.

A key step in the proposed reaction mechanism is reaction 15 between $(SCN)_2^-$ and ONSCN, for which the rate constant, k_{15}, could range from 2×10^5 to 5×10^8 $M^{-1}s^{-1}$ depending on the magnitude of K_{14}. This reaction could be interpreted as the S-nitrosation of $(SCN)_2^-$ by ONSCN, wherein NO^+ transfers from ONSCN to one of the sulfur atoms of $(SCN)_2^-$, presumably forming an unstable intermediate species $ON(SCN)_2$ which rapidly decomposes to NO and $(SCN)_2$. Alternatively, the reaction could be interpreted as a substitution of the $(SCN)_2^-$ radical for NO in ONSCN, releasing NO and forming $(SCN)_3^-$, which persists in equilibrium with $(SCN)_2$ and SCN^-.[34] It is of interest to compare the magnitude of k_{15} suggested in this study to the rate constants of nitrosation reactions involving ONSCN to determine if the required values of k_{15} are plausible. In the case of S-nitrosation, the high reactivity of many substrates makes it impossible to determine the rate constant, as is the case for the reaction between ONSCN and a range of heterocyclic thiones,[12] while the reaction of ONSCN with mercapto-carboxylic acids occurs with a rate constant of $\sim 1 \times 10^4$ $M^{-1}s^{-1}$. In the case of N-nitrosation, the rate constant for the reaction between ONSCN and aniline and several primary amino acids[43] is $\sim 1 \times 10^8$ $M^{-1}s^{-1}$, while a range of aniline derivatives react with rate constants between 1×10^5 and 5×10^8 $M^{-1}s^{-1}$. Thus, the rate constants required for reaction 15 in the proposed mechanism lie within the range of values typically encountered for nitrosation reactions effected by ONSCN. In the case of the substitution of the $(SCN)_2^-$ radical for NO in ONSCN, the analogous reactions between thiyl radicals and thionitrites are reportedly barrierless,[44] suggesting a reaction rate close to the diffusion controlled limit. Reactions 18 and 27, which offer alternate pathways for the consumption of $(SCN)_2^-$, do not have a significant impact on the kinetics. Although the rate constant for reaction 27 is large, it is second order in $(SCN)_2^-$, the concentration of which is low (i.e., due to the low value of K_{14}) and as such the rate of this reaction remains insignificant compared with the rate of reaction 15.

Pathway 2 - Reaction 5. This pathway comprises a second order reaction in ONSCN, directly generating NO and $(SCN)_2$. Evidence supporting this reaction includes the tendency of ONSCN decomposition kinetics to approach a second order reaction in the later stages (conditions whereby the accumulation of NO in the solution suppresses reaction 14) and the fact that inclusion of this reaction in kinetic simulations leads to a substantially improved fit to the data. Other related systems, including the decomposition of nitroso-thiourea[35,36] and the oxidation of iodide ions by HNO_2[42,45] (which likely proceeds through an ONI intermediate) contain a term in the initial rate that is second order in nitroso species. Hence, it stands to reason that a similar mechanism operates for ONSCN.

Pathway 3 - (iii) Formation and decomposition of ONOSCN – Reactions 21-23. Pathways 1 and 2 proceed too slowly to account for the observed rate of decomposition at thiocyanate concentrations below 0.2 M, indicating that an additional reaction pathway must operate under these conditions. We propose the formation and decomposition of a new species, ONOSCN, to account for the kinetics of ONSCN decomposition under conditions of relatively low thiocyanate ion concentration. In the proposed mechanism, ONOSCN arises as a consequence of the reaction of ONSCN with HOSCN, and decomposes via homolysis forming nitric oxide and OSCN. The magnitude of K_{ONOSCN} indicates that only a small fraction of HOSCN converts into ONOSCN. The combination of OSCN and NO was assumed to occur rapidly with a rate constant of 4.3×10^9 $M^{-1}s^{-1}$, which falls in the range of rate constants reported in the literature for reactions between NO and a variety of radicals, including $(SCN)_2^-$, $(Br)_2^-$, CO_3^-,[37] organic peroxyl radicals[46] and thiyl radicals[47] that all occur with rate in excess of 10^9 $M^{-1}s^{-1}$. Formation of OSCN has previously been proposed to account for the complex kinetics associated with oxidation of SCN^- by ClO_2.[33] That study assumed that OSCN undergoes dimerization and hydrolysis with a rate constant of 1×10^7 $M^{-1}s^{-1}$ (i.e., k_{23}), which coincides reasonably well with the value of 1.7×10^7 $M^{-1}s^{-1}$ determined in the present study. Experimentation with different values of k_{23} in the simulations showed that the previously reported value could be accommodated by making appropriate changes to K_{21} and k_{22} with no reduction in the goodness of fit. Numerous intermediates contribute to the hydrolysis of $(SCN)_2$ and it is plausible that they too participate in reactions with nitrous acid or nitrosyl thiocyanate. However, owing to the large rate constants for their consumption,[33] the concentration of such intermediates (e.g., HO_2SCN, HO_3SCN) is predicted to be low, resulting in minimal contributions from these reactions.

Formation of N_2O. Small amounts of N_2O arise in the product gases at levels of less than 3%, as confirmed both by FTIR and MIMS. Because of its low abundance and subsequently insignificant impact on the overall decomposition kinetics, we did not attempt to model the formation of this species. A potential pathway for the formation of N_2O involves the decomposition of nitrosyl cyanide, ONCN, which reportedly hydrolyzes to produce N_2O and CO_2.[48] Cyanide ions, formed via the hydrolysis of $(SCN)_2$ (generated from the decomposition of ONSCN) could react with nitrous acid to produce ONCN, in the same way as thiocyanate ions react with nitrous acid to form nitrosyl thiocyanate. An alternative pathway may consist of ONSCN hydrolyzing

dx.doi.org/10.1021/ic102445d |Inorg. Chem. 2011, 50, 7440–7452

to form ONH, leading to formation of N_2O (via combination of ONH[49]).

$$ONCN + 2H_2O \rightleftharpoons ONH + CO_2 + NH_3 \quad (32)$$

$$ONSCN + H_2O \rightleftharpoons ONH + HOSCN \quad (33)$$

$$2ONH \rightarrow N_2O + H_2O \quad (34)$$

CONCLUSIONS

The mechanism of the decomposition of nitrosyl thiocyanate involves a complex system of reactions, with the rate suppressed by the accumulation of the product, nitric oxide, and catalyzed by thiocyanate ions. We examined potential reaction mechanisms by fitting the kinetic parameters to the experimental measurements, and subjected these kinetic parameters to thermodynamic and kinetic scrutiny, to identify three parallel pathways for the decomposition of ONSCN. The first two pathways, which describe the kinetics at high thiocyanate ion concentrations comprise a reaction that is second order in ONSCN to generate NO and $(SCN)_2$ and a reaction between ONSCN and SCN^- to form NO and $(SCN)_2^-$, with the latter pathway being reversible. The rate limiting step in the mechanism corresponds to the consumption of $(SCN)_2^-$ radicals by ONSCN, which could occur via either radical substitution or S-nitrosation. The third reaction pathway, which becomes significant at low thiocyanate concentrations, involves the formation of a previously unreported species, ONOSCN, via reaction between ONSCN and HOSCN, the latter being an intermediate in the hydrolysis of $(SCN)_2$. ONOSCN contributes to NO formation via homolysis of the O−NO bond and subsequent dimerization and hydrolysis of OSCN. The proposed kinetic mechanism provides an excellent fit to the experimental measurement, allowing the rate of NO formation from the decomposition of ONSCN to be modeled accurately.

ASSOCIATED CONTENT

Supporting Information. Kinetic data for ONSCN decomposition, typical UV−vis and FTIR spectra. This material is available free of charge via the Internet at http://pubs.acs.org.

AUTHOR INFORMATION

Corresponding Author

*Phone: +61 2 4985-4433. Fax: +61 2 4921-6893. E-mail: Bogdan.Dlugogorski@newcastle.edu.au.

ACKNOWLEDGMENT

We acknowledge the Australian Research Council and Dyno Nobel Asia Pacific Pty Ltd. for funding the research and Ms. Wendy Venpin for assistance with membrane inlet mass spectrometry experiments. M.S.R. thanks The University of Newcastle for a Research Higher Degree Scholarship.

REFERENCES

(1) Hunger, K.; Mischke, P.; Rieper, W.; Raue, R.; Kunde, K.; Engel, A. *Azo Dyes*; Wiley-VCH Verlag GmbH & Co. KGaA, 2000.
(2) Rollefson, G. K.; Oldershaw, C. F. *J. Am. Chem. Soc.* **1932**, *54*, 977–979.
(3) da Silva, G.; Dlugogorski, B. Z.; Kennedy, E. M. *AIChE J.* **2006**, *52*, 1558–1565.
(4) Nguyen, D. A.; Iwaniw, M. A.; Fogler, H. S. *Chem. Eng. Sci.* **2003**, *58*, 4351–4362.
(5) Stamler, J. S.; Singel, D. J.; Loscalzo, J. *Science* **1992**, *258*, 1898–1902.
(6) Williams, D. L. H. *Acc. Chem. Res.* **1999**, *32*, 869–876.
(7) Choi, J.; Valentine, R. L. *Environ. Sci. Technol.* **2003**, *37*, 4871–4876.
(8) Walse, S. S.; Mitch, W. A. *Environ. Sci. Technol.* **2008**, *42*, 1032–1037.
(9) Wu, H.; Loeppky, R. N.; Glaser, R. *J. Org. Chem.* **2005**, *70*, 6790–6801.
(10) Ridd, J. H. *Q. Rev., Chem. Soc.* **1961**, *15*, 418–441.
(11) Meyer, T. A.; Williams, D. L. H. *J. Chem. Soc., Perkin Trans. 2* **1988**, 517–521.
(12) Amado, S.; Blakelock, L.; Holmes, A. J.; Williams, D. L. H. *J. Chem. Soc., Perkin Trans. 2* **2001**, 441–447.
(13) Hughes, E. D.; Ridd, J. H. *J. Chem. Soc.* **1958**, 82–88.
(14) Francisco, V.; Garcia-Rio, L.; Antonio Moreira, J.; Stedman, G. *New J. Chem.* **2008**, *32*, 2292–2298.
(15) Garley, M. S.; Stedman, G. *J. Chem. Res.* **1996**, 9.
(16) Williams, D. L. H. *Nitrosation Reactions and the Chemistry of Nitric Oxide*; Elsevier B. V.: Amsterdam, 2004.
(17) Stedman, G.; Whincup, P. A. E. *J. Chem. Soc.* **1963**, 5796–5799.
(18) Bourne, N. K.; Field, J. E. *Proc. R. Soc. London, Ser. A* **1991**, *435*, 423–435.
(19) Lecher, H.; Graf, F. *Ber. Dtsch. Chem. Ges. B* **1926**, *59B*, 2601–2.
(20) Doherty, A. M.; Garley, M. S.; Haine, N.; Stedman, G. *J. Chem. Soc., Dalton Trans.* **1997**, 2163–2166.
(21) Jones, E.; Munkley, C. G.; Phillips, E. D.; Stedman, G. *J. Chem. Soc., Dalton Trans.* **1996**, 1915–1920.
(22) Bazsa, G.; Epstein, I. R. *Int. J. Chem. Kinet.* **1985**, *17*, 601–612.
(23) Nagy, P.; Lemma, K.; Ashby, M. T. *Inorg. Chem.* **2007**, *46*, 285–292.
(24) Bunton, C. A.; Dahn, H.; Loewe, L. *Nature* **1959**, *183*, 163–165.
(25) Armor, J. N. *J. Chem. Eng. Data* **1974**, *19*, 82–84.
(26) Tu, C.; Swenson, E. R.; Silverman, D. N. *Free Radical Biol. Med.* **2007**, *43*, 1453–1457.
(27) Kuzmic, P. *Anal. Biochem.* **1996**, *237*, 260–273.
(28) da Silva, G. R.; Dlugogorski, B. Z.; Kennedy, E. M. *Int. J. Chem. Kinet.* **2007**, *39*, 645–656.
(29) Barnett, J. J.; McKee, M. L.; Stanbury, D. M. *Inorg. Chem.* **2004**, *43*, 5021–5033.
(30) Schwartz, S. E.; White, W. H. *Adv. Environ. Sci. Technol.* **1983**, *12*, 1–116.
(31) Stedman, G.; Whincup, P. A. E. *J. Chem. Soc.* **1969**, 1945–1948.
(32) Figlar, J. N.; Stanbury, D. M. *Inorg. Chem.* **2000**, *39*, 5089–5094.
(33) Figlar, J. N.; Stanbury, D. M. *J. Phys. Chem. A* **1999**, *103*, 5732–5741.
(34) Barnett, J. J.; Stanbury, D. M. *Inorg. Chem.* **2002**, *41*, 164–166.
(35) Collings, P.; Garley, M. S.; Stedman, G. *J. Chem. Soc., Dalton Trans.* **1981**, 331–335.
(36) Garley, M. S.; Stedman, G.; Miller, H. *J. Chem. Soc., Dalton Trans.* **1984**, 1959–1963.
(37) Czapski, G.; Holcman, J.; Bielski, B. H. J. *J. Am. Chem. Soc.* **1994**, *116*, 11465–11469.
(38) Milosavljevic, B. H.; LaVerne, J. A. *J. Phys. Chem. A* **2005**, *109*, 165–168.
(39) Neta, P.; Huie, R. E.; Ross, A. B. *J. Phys. Chem. Ref. Data* **1988**, *17*, 1027–1284.
(40) Park, J. Y.; Lee, Y. N. *J. Phys. Chem.* **1988**, *92*, 6294–302.
(41) Huie, R. E.; Neta, P. *J. Phys. Chem.* **1986**, *90*, 1193–1198.
(42) Dózsa, L.; Szilassy, I.; Beck, M. T. *Inorg. Chim. Acta* **1976**, *17*, 147–153.
(43) da Silva, G.; Kennedy, E. M.; Dlugogorski, B. Z. *J. Am. Chem. Soc.* **2005**, *127*, 3664–3665.
(44) Stamler, J. S.; Toone, E. J. *Curr. Opin. Chem. Biol.* **2002**, *6*, 779–785.

(45) Ferranti, F.; Indelli, A. *Gazz. Chim. Ital.* **1980**, *110*, 273–277.
(46) Goldstein, S.; Lind, J.; Merenyi, G. *J. Phys. Chem. A* **2004**, *108*, 1719–1725.
(47) Madej, E.; Folkes, L. K.; Wardman, P.; Czapski, G.; Goldstein, S. *Free Radical Biol. Med.* **2008**, *44*, 2013–2018.
(48) Shirota, F. N.; Goon, D. J. W.; DeMaster, E. G.; Nagasawa, H. T. *Biochem. Pharmacol.* **1996**, *52*, 141–147.
(49) Bazylinski, D. A.; Hollocher, T. C. *Inorg. Chem.* **1985**, *24*, 4285–4288.